doi:10.1093/brain/awv047 BRAIN 2015: 138; 1284–1296 | 1284

BRAIN
A JOURNAL OF NEUROLOGY

The integrative role of the pedunculopontine nucleus in human gait

Brian Lau,[1] Marie-Laure Welter,[1,2] Hayat Belaid,[2] Sara Fernandez Vidal,[1,3] Eric Bardinet,[1,3] David Grabli[1,2] and Carine Karachi[1,2]

See Windels *et al.* for a scientific commentary on this article (doi:10.1093/brain/awv059).

The brainstem pedunculopontine nucleus has a likely, although unclear, role in gait control, and is a potential deep brain stimulation target for treating resistant gait disorders. These disorders are a major therapeutic challenge for the ageing population, especially in Parkinson's disease where gait and balance disorders can become resistant to both dopaminergic medication and subthalamic nucleus stimulation. Here, we present electrophysiological evidence that the pedunculopontine and subthalamic nuclei are involved in distinct aspects of gait using a locomotor imagery task in 14 patients with Parkinson's disease undergoing surgery for the implantation of pedunculopontine or subthalamic nuclei deep brain stimulation electrodes. We performed electrophysiological recordings in two phases, once during surgery, and again several days after surgery in a subset of patients. The majority of pedunculopontine nucleus neurons (57%) recorded intrasurgically exhibited changes in activity related to different task components, with 29% modulated during visual stimulation, 41% modulated during voluntary hand movement, and 49% modulated during imaginary gait. Pedunculopontine nucleus local field potentials recorded post-surgically were modulated in the beta and gamma bands during visual and motor events, and we observed alpha and beta band synchronization that was sustained for the duration of imaginary gait and spatially localized within the pedunculopontine nucleus. In contrast, significantly fewer subthalamic nucleus neurons (27%) recorded intrasurgically were modulated during the locomotor imagery, with most increasing or decreasing activity phasically during the hand movement that initiated or terminated imaginary gait. Our data support the hypothesis that the pedunculopontine nucleus influences gait control in manners extending beyond simply driving pattern generation. In contrast, the subthalamic nucleus seems to control movement execution that is not likely to be gait-specific. These data highlight the crucial role of these two nuclei in motor control and shed light on the complex functions of the lateral mesencephalus in humans.

1 Sorbonne Universités, UPMC Univ Paris 06, UMR S 1127, CNRS UMR 7225, ICM, F-75013, Paris, France
2 Assistance Publique-Hôpitaux de Paris, Groupe Hospitalier Pitié-Salpêtrière, 47 boulevard de l'Hôpital, 75013 Paris, France
3 Centre de Neuroimagerie de Recherche, Institut du Cerveau et de la Moelle épinière, F-75013, Paris, France

Correspondence to: Brian Lau,
Institut du Cerveau et de la Moelle épinière
UMR S 1127, CNRS UMR 7225
Hôpital de la Pitié Salpêtrière
47 Bd de l'Hôpital
75013, Paris, France
E-mail: brian.lau@upmc.fr

Keywords: pedunculopontine nucleus; subthalamic nucleus; Parkinson's disease; deep brain stimulation; gait

Abbreviations: DBS = deep brain stimulation; PPN = pedunculopontine nucleus; STN = subthalamic nucleus

Received October 12, 2014. Revised December 11, 2014. Accepted January 6, 2015. Advance Access publication March 12, 2015

Introduction

Moving through the environment is a crucial and highly evolved ability in vertebrates, which humans primarily accomplish using the unique capacity to walk on two legs. This ability is controlled by neural networks linking automatic pattern generators in the spinal cord with supraspinal brainstem and forebrain structures responsible for selecting, initiating and regulating locomotor behaviour (Orlovsky *et al.*, 1999). The brainstem lateral mesencephalus is a highly conserved supraspinal locomotor centre that has been identified in vertebrates ranging from lampreys to primates (Le Ray *et al.*, 2011), and includes the pedunculopontine (PPN) and cuneiform nuclei. The PPN is a complex structure divided into a pars compacta containing mainly cholinergic neurons and a pars dissipata containing glutamatergic and GABAergic neurons (Olszewski and Baxter, 1954). The pedunculopontine and cuneiform nuclei receive direct cortical inputs, and are well positioned to influence locomotor behaviour via ascending outputs to the basal ganglia and thalamus (Pahapill and Lozano, 2000), as well as via descending outputs to the spinal cord (Rolland *et al.*, 2011).

The brainstem region containing the pedunculopontine and cuneiform nuclei is commonly referred to as the mesencephalic locomotor region based on observations that electrical stimulation of this region can initiate and modulate locomotion in animals (Shik *et al.*, 1966; Eidelberg *et al.*, 1981; Skinner and Garcia-Rill, 1984; Mori *et al.*, 1989), and that chemical modulation (Takakusaki *et al.*, 2003) as well as lesioning cholinergic PPN neurons in monkeys (Karachi *et al.*, 2010) impairs gait. The mesencephalic locomotor region is modulated by changes in imagined locomotion in healthy humans (Jahn *et al.*, 2008; Karachi *et al.*, 2012), which also modulates cortical networks similar to those involved during real gait (La Fougère *et al.*, 2010). Further evidence implicating the mesencephalic locomotor region in locomotor control comes from pathophysiological studies of gait and balance disorders, which are major causes of chronic disability and mortality in the elderly (Snijders *et al.*, 2007), suggesting that PPN dysfunction may be key to understanding the pathophysiology of gait disorders resistant to dopaminergic treatment (Pahapill and Lozano, 2000; Snijders *et al.*, 2007; Demain *et al.*, 2014).

In Parkinson's disease, dopamine replacement therapy and deep brain stimulation (DBS) of the subthalamic nucleus (STN) effectively treat tremor, rigidity and akinesia caused by dopamine cell death (Limousin *et al.*, 1998). These interventions can also effectively treat DOPA-sensitive gait and balance disorders, but as Parkinson's disease advances gait disorders can become resistant to dopamine medication and STN-DBS (Grabli *et al.*, 2012), which may be related to degeneration of cholinergic neurons in the PPN (Hirsch *et al.*, 1987; Jellinger, 1988; Zweig *et al.*, 1989). This is associated with decreased thalamic cholinergic activity, and both brainstem cholinergic loss and decreases in thalamic cholinergic activity correlate with the history of falls in patients with advanced Parkinson's disease (Bohnen *et al.*, 2009; Karachi *et al.*, 2010). Functional imaging in patients with Parkinson's disease indicates that PPN area activity depends on the severity of gait disorders, where blood oxygenation level-dependent enhancement during imaginary gait may reflect compensation for brainstem atrophy observed in patients with gait disorders (Snijders *et al.*, 2011; Demain *et al.*, 2014; Maillet *et al.*, 2015).

Deep brain stimulation of the PPN has recently been tested for treating severe dopamine-resistant gait disorders in patients with Parkinson's disease, using stimulation parameters thought to stimulate the remaining neurons (Mazzone *et al.*, 2005; Plaha and Gill, 2005; Stefani *et al.*, 2007; Ferraye *et al.*, 2010; Moro *et al.*, 2010). Electrophysiological recordings performed in these patients during DBS surgery have revealed that some PPN neurons respond to behavioural manipulations intended to elicit locomotor contexts, including alternating leg movements (Piallat *et al.*, 2009) and imaginary gait (Tattersall *et al.*, 2014). While these results are consistent with a role for the mesencephalic locomotor region in controlling locomotion, it remains unclear how neural activity in the human mesencephalic locomotor region relates to sensory perception and the selection, initiation and modulation of motor programs supporting locomotion.

We sought to improve understanding of the role of the PPN in gait control by recording neural activity in this nucleus in patients with Parkinson's disease undergoing DBS surgery for intractable gait disorders. We used a validated imaginary gait task (Bakker *et al.*, 2007; Karachi *et al.*, 2012) and compared PPN neural activity to STN recordings made in a second group of patients with Parkinson's disease performing this same task. We provide the first comparative analysis of the neural activity of these two nuclei in a locomotor context, and our results suggest distinct roles for the PPN and STN in locomotor control.

Materials and methods

Patients

Fourteen patients with idiopathic Parkinson's disease were recruited at the Pitié-Salpêtrière Hospital. We included eight patients using standard criteria for STN-DBS (Welter *et al.*, 2002). For PPN-DBS, we included six patients using the same criteria except that gait and balance disorders measured by freezing of gait and/or falling subscores were $\geqslant 2$ ON DOPA (Tables 1 and 2). Thus, patients in the PPN-DBS group exhibited significantly more DOPA-resistant gait disorders compared to the STN-DBS group. Patients in each group participated in separate clinical trials that were approved by the local ethical committee of the Salpêtrière Hospital and the INSERM-DGOS (PPN trial #NCT02055261, STN trial #NCT01682668). Randomization

Table 1 Demographic and clinical features of patients

	Gender, Age	Disease duration	Activities of daily living (UPDRS II)		Motor disability (UPDRS III)		Levodopa motor complications	Levodopa-equivalent dosage	Cognitive status			
			OFF	ON	OFF	ON			MMS	MDRS	Frontal score	WCST
PPN-DBS												
S01	M, 69	19	21	19	44	18	4	1700	28	132	47	12
S02	F, 70	18	26	9	45	16	9	570	25	140	52	15
S03	F, 68	23	28	19	61	30	9	700	29	130	51	12
S04	F, 64	10	22	6	38	19	4	1050	25	141	52	12
S05	M, 63	14	11	11	38	16	5	585	29	139	54	20
S06	M, 46	12	22	5	50	19	10	1300	27	139	58	20
Mean (SD)	63 (8.9)	16 (4.9)	22 (5.9)	12 (6.2)	46 (8.6)	20 (5.2)	7 (2.8)	984 (453)	27 (1.9)	137 (4.6)	52 (3.6)	15 (3.9)
STN-DBS												
S07	M, 55	9	17	14	18	3	5	1000	30	143	59.5	20
S08	F, 53	7	33	7	46	11	8	1130	27	143	60	20
S09	F, 51	13	15	1	32	1	6	450	30	144	60	20
S10	M, 55	11	24	16	53	11	7	625	25	122	46	12
S11	F, 57	10	24	2	26	4	9	875	29	143	54	15
S12	M, 60	10	25	11	53	27	8	1080	28	144	58	20
S13	F, 58	11	35	11	58	17	7	400	30	144	58	20
S14	F, 67	10	18	2	37	15	5	1125	28	129	44	9
Mean (SD)	57 (4.9)	10 (1.7)*	24 (7.3)	8 (5.9)	40 (14.3)	11 (8.6)*	7 (1.5)	836 (303)	28 (1.8)	139 (8.6)	55 (6.4)	17 (4.4)

*$P < 0.05$ unpaired *t*-test comparing STN-DBS patients with PPN-DBS; MMS = Mini-Mental Status (range 0–30, higher score indicates better cognitive function); MDRS = Mattis Dementia Rating Scale (range 0–144, higher score indicates better cognitive function); UPDRS = Unified Parkinson's Disease Rating Scale (part II: range 0–52; part III: range 0–108; part IV: range 0–44; higher scores indicate worse parkinsonian status); WCST = Wisconsin Card Sorting Test (range 0–20; higher scores indicate better cognitive status). OFF and ON refer to dopaminergic medication.

was not used to assign patients, and the authors were not blinded to the group allocations. All patients agreed to participate and signed a written consent.

Imagery tasks

Imaginary gait task

Patients performed an imaginary gait task previously described (Karachi *et al.*, 2012). Prior to surgery, patients were trained to walk along an 8-m long segment of a corridor. On separate trials they were instructed to walk at normal speed and then 30% faster. After practicing walking at each speed, patients were seated in front of a computer screen and trained to perform the imaginary gait task. Each trial began with the presentation of a white cross at the centre of the screen. After a delay, an image showing the corridor that the patient had walked along was displayed, along with instructions indicating the speed at which to imagine gait (normal or rapid, pseudo-randomized). When the patient was ready, he closed his eyes and initiated imaginary gait by pressing a button. Finally, the patient terminated imagery with a second button press, and then opened his eyes.

Imaginary object movement task

Patients in the PPN-DBS group were also trained on an imaginary object movement task where they imagined an object moving at two different speeds along the same 8-m corridor segment. These conditions were indicated by 'normal object' and 'rapid object'. The trials were otherwise identical in terms of stimulus presentation, times and the sequence of button pressing and eye closing the subject was instructed to perform to initialize and terminate imagery.

During surgery, patients only performed the imaginary gait task due to time limitations. In postsurgical sessions, four PPN patients performed both imaginary gait and object movement tasks (conditions pseudo-randomly interleaved).

Surgical procedure and localization of neurons and definitive DBS electrodes

We targeted the PPN and STN using a combination of direct MRI targeting (Bejjani *et al.*, 2000; Zrinzo *et al.*, 2008) and a 3D histological atlas of the basal ganglia that were deformed to the preoperative T_1 MRI of each patient's brain obtained the day before surgery (Yelnik *et al.*, 2007). We obtained a set of coordinates with each method, aiming for the lowest contact to be just outside the lower limit of the nucleus, and defined a target for each side by averaging these coordinates. We chose trajectories that avoided ventricles, the caudate nuclei, and blood vessels, and accounted for the size of the brainstem (for PPN surgeries). During surgery, we used a Leksell frame (Elekta Instruments, Inc.) with X-ray imaging to control the position of the electrodes. For PPN recordings, we used only two microelectrodes (instead of three to five) per side to reduce haemorrhagic risk. For STN recordings, we used three microelectrodes for both sides. Individual neurons were localized within the structures using preoperative MRI and perioperative X-rays to validate microelectrode

Table 2 Gait and balance disorders of patients

	Falling (item 13-UPDRS II)		FOG (item 14-UPDRS II)		Axial motor score (UPDRS III)		Postural stability (item 29-UPDRS III)		Gait (item 30-UPDRS III)	
	OFF	ON	OFF	ON	OFF	ON	OFF	ON	OFF	ON
PPN-DBS										
S01	4	4	4	4	8	2	2	1	3	1
S02	2	2	3	2	12	6	3	2	3	2
S03	2	2	3	3	11	8	3	1	3	3
S04	2	2	3	1	8	3	2	1	3	1
S05	2	2	3	3	4	4	2	1	2	2
S06	2	2	3	2	9	1	2	2	3	0
Mean (SD)	2 (0.8)	2 (1.2)	3 (0.4)	2 (1.0)	9 (2.8)	4 (2.6)	2 (0.5)	1 (0.5)	3 (0.4)	2 (1.0)
STN-DBS										
S07	0	0	0	0	0	0	0	0	0	0
S08	0	0	3	0	14	2	2	0	4	0
S09	0	0	0	0	3	0	1	0	1	0
S10	0	0	0	0	3	0	1	0	1	0
S11	0	0	3	0	3	0	0	0	1	0
S12	2	0	3	1	11	5	2	0	4	1
S13	1	0	4	1	11	3	1	0	3	1
S14	0	0	0	0	10	4	0	0	2	0
Mean (SD)	0 (0.7)*	0 (0)*	2 (1.8)*	0 (0.5)*	7 (5.2)	2 (0.1)	1 (0.8)*	0 (0)*	2 (1.5)	0 (0.5)*

*$P < 0.05$ unpaired *t*-test comparing STN-DBS patients with PPN-DBS; UPDRS = Unified Parkinson's Disease Rating Scale [part II: Falling and freezing of gait (FOG) scores: range 0–4; part III: axial score: range 0–20; gait and postural instability scores: range 0–4; higher scores indicate worse parkinsonian status]. OFF and ON refer to dopaminergic medication.

trajectories and depths. We localized the definitive DBS electrodes for each patient using a postoperative helicoidal CT scan registered to the preoperative T_1-weighted MRI (Bardinet *et al.*, 2009).

Data collection

The patient was brought out of anaesthesia, and tungsten microelectrodes (1 MΩ impedance; FHC Inc.) were lowered together using a microdrive. We started physiological recordings 5 mm above the target. We reminded patients of the imaginary gait task, which was presented on a mounted LCD screen. When neural activity could be stably recorded, the patients performed the task for ~15 min, using the hand contralateral to the recorded PPN or STN to press the button. Patients were free to discontinue the experiment at any time. After finishing the task and the clinical assessments, the patient was re-anaesthetized and the definitive DBS electrode was implanted. This entire procedure was repeated for the other hemisphere.

Neuronal activity was amplified, filtered and written to disk for offline analysis (Guideline 4000, FHC Inc. or Leadpoint, Medtronic). Action potentials were isolated using manual clustering on the basis of several waveform parameters including principal components, peak and trough amplitudes, as well as the presence of a refractory period (Offline Sorter, Plexon Instruments). We characterized over half of the unit activities as single-unit, with signal-to-noise ratios >4 (Tattersall *et al.*, 2014) (PPN, $n = 27$, mean signal-to-noise ratio = 6.01, min signal-to-noise ratio = 4.14; STN, $n = 36$, mean signal-to-noise ratio = 6.34, min signal-to-noise ratio = 4.30). When multiple action potentials could not be separated into well-defined clusters, we thresholded the raw voltage signal at ~3 standard deviations (SD) from the mean and labelled this multi-unit activity (PPN, $n = 22$, mean signal-to-noise ratio = 3.43, min signal-to-noise ratio = 3.01; STN, $n = 31$, mean signal-to-noise ratio = 3.39, min signal-to-noise ratio = 2.81). There was no difference in the proportion of single-units isolated in each area ($P > 0.5$), nor in the signal-to-noise ratios between areas (*P*-values > 0.4).

Postsurgical recordings were made 4 days after surgery for PPN patients. Local field potentials were recorded bilaterally from the definitive DBS electrodes (model 3389, Medtronic Neurological Division), which had four cylindrical platinum-iridium cylindrical contacts (1.27 mm in diameter and 1.5 mm in length) separated by 0.5 mm. Signals were amplified, low pass filtered at 250 Hz and digitized at 512 Hz (Basis BE System, EB Neuro S.p.A.). Bipolar recordings were made between adjacent contacts of each electrode, yielding six recording channels per patient (three per side). Patients were on their dopaminergic medication, and were comfortably seated in front of a screen to perform the imagery tasks for ~30 min. Five patients participated in the postsurgical local field potential recordings. We excluded data from two of these patients; one due to excessive signal artefacts, and the second patient could not perform the task due to postsurgical fatigue. Local field potentials were processed to remove power line noise by fitting a parametric function to the power spectral density of the raw voltage signal in the vicinity of 50 Hz (±2 Hz). The raw voltage signal was then filtered using the inverse of the fitted function so that the resulting spectrum at 50 Hz was similar to that of surrounding frequencies (Zanos *et al.*, 2011). We excluded data from individual trials when the amplitude of the raw voltage signal exceeded 500 μV or 6 SD of the amplitude distribution across the session.

Data analysis

We performed all analyses using MATLAB (version 2013a, Mathworks Inc.) and R (version 3.10, R Core Development Team). We fit the linear mixed models described below using the R package lme4 (version 1.1), and assessed significance with mixed-effects ANOVAs using the R package lmerTest (version 2.0) with Satterthwaite's approximation for the denominator degrees of freedom of the F-statistic.

Behavioural analyses

We analysed the durations between button presses initiating and terminating imagery. Trials where this duration was <2 or >30 s were excluded, leaving 1463 (97.5%) trials of intrasurgical data and 577 (96.7%) trials of postsurgical data for analysis. We modelled imagination duration using a linear mixed model, including fixed effects of target location (PPN or STN), speed (rapid or normal) and imagery type (gait or object movement), with an additive random effect for each patient. Imagination time distributions were positively skewed, and we log-transformed the data to symmetrize and stabilize residuals. Resulting model residuals were symmetrically distributed, but had heavier than Gaussian tails. We checked that this did not affect our conclusions by fitting robust versions of the models (robustlmm version 1.6), and confirmed that our conclusions were unchanged.

Analysis of spiking activity

We compared activity within a trial to baseline using a Wilcoxon rank sum test. The activity for every trial of each neuron was first smoothed using a Gaussian kernel density estimator with optimal bandwidth (Shimazaki and Shinomoto, 2010). We estimated baseline rate by averaging activity from -2.5 to -0.1 s before visual instruction onset for each trial, and compared activity at every millisecond to this baseline distribution. We adjusted for multiple comparisons using the procedure of Benjamini and Hochberg (1995) to control the false discovery rate (FDR).

We quantified modulation strength in three time windows (Visual, 0 to 0.5 s after visual instruction onset; Motor, -0.5 to 0.5 s relative to button presses; Imaginary gait, 2 to 4 s after imagery was initiated), z-scoring absolute responses by subtracting mean baseline activity and dividing by its standard deviation (baseline from -2.5 to -0.1 s before visual instruction onset). We modelled modulation strength using a linear mixed model, including fixed effects of target location (PPN or STN), recording side (right or left) and recording depth, with an additive random effect for each patient. Distributions of the resulting model residuals were positively skewed, and we checked that this did not affect our conclusions by power transforming modulation strength to symmetrize and stabilize residuals. This yielded residuals that were Gaussian (Lilliefors test) with homogeneous variance across patients (Levene's test). The results from these fits agreed with those presented in the 'Results' section; PPN modulation strength was significantly greater than STN modulation strength in the Visual ($P = 0.031$) and Imaginary gait ($P = 0.037$) epochs, but not the Motor epoch ($P = 0.367$).

Comparing recording locations

We compared the anatomical localization of neurons with different response properties by treating the location of each neuron (x, y, z position) as a sample, and testing for differences between sample distributions non-parametrically using a test based on statistical energy (Székely and Rizzo, 2013). P-values were calculated by bootstrap.

Time-frequency analysis

We estimated spectral power as a function of time and frequency using a multi-taper estimation algorithm (Mitra and Bokil, 2007) implemented in the Chronux library (version 2.10, http://chronux.org). For each bipolar local field potential recording, power was calculated in 500 ms windows stepped by 30 ms, using five orthogonal tapers with a time-bandwidth product equal to 3. Spectrograms were normalized to the average baseline spectrum measured -3 to -1 s before visual instruction onset, and transformed to decibels. We quantified changes in the same three time windows we used to analyse spiking data, modelling spectral modulations with a linear mixed model that included fixed effects of recording depth (dorsal, intermediate or ventral), imagination speed (rapid or normal), imagination type (gait or object movement) and recording side (right or left), with an additive random effect for each patient. Resulting model residuals were symmetrically distributed, but had heavier than Gaussian tails. We checked that this did not affect our conclusions by fitting robust versions of the models, and confirmed that our conclusions were unchanged.

Results

Behavioural performance

We trained 14 patients with Parkinson's disease to perform an imaginary gait task 1 month before and again the day prior to DBS surgery. Each trial consisted of viewing an instruction on a screen and pressing a button to initiate and terminate an epoch of gait imagination with the eyes closed. Patients were instructed to imagine walking down a corridor they were familiar with, and they practiced both real and imaginary gait until they reliably produced shorter imagination times when instructed to imagine walking faster compared to walking at a normal speed. They performed this task when brought out of anaesthesia during DBS surgery while we recorded the spiking activity of neurons in the PPN or STN using microelectrodes (intrasurgical), and in a subset of PPN patients 4 days later while we recorded local field potentials from the implanted DBS macroelectrodes (postsurgical). Patients successfully performed the imagery tasks, producing shorter imagination times when instructed to imagine walking faster compared to normal walking speed, both intrasurgically (7.26 s versus 8.75 s, $P < 0.001$) and postsurgically (7.55 s versus 8.88 s, $P < 0.001$). Imagination times did not depend on patient group (PPN versus STN, $P > 0.4$), and all patients except

one in the STN group produced shorter imagination times during rapid compared to normal speed trials. For the post-surgical recordings, patients also imagined object motion at two different speeds, and their performance in these trials was not different from imaginary gait trials ($P > 0.8$). Thus, both patient groups performed imagery gait similarly, despite differences between patient groups during real gait (Table 2).

PPN and STN neurons respond differently during imaginary gait

We recorded 49 single- or multi-units in the PPN of five patients and 67 single- or multi-units in the STN of eight patients. Figure 1A illustrates a range of task-related activity that we observed in individual neurons in the PPN and STN, including modulations during imaginary gait, visual instruction, and the physical movements (button presses) initiating and terminating imaginary gait. We summarized the prevalence of task-related changes by comparing activity at each point in time throughout the trial to baseline activity before visual stimulus presentation, pooling significance across neurons within each nucleus (Fig. 1B). There were substantially more modulated neurons in the PPN compared to the STN, which was evident beginning with visual instruction presentation and was maintained until patients terminated imaginary gait. In contrast, there were relatively few modulated neurons in the STN; significant changes from baseline occurred primarily around the time of button presses, and significant changes during imaginary gait were less coherent across the population. For both PPN and STN neurons, we occasionally observed small differences between the rapid and normal speed conditions, but we found fewer than 5% significant differences at any point in time when comparing these conditions, and we therefore pooled the data for all analyses.

Individual neural responses within both the PPN and the STN could exhibit positive or negative modulations relative to baseline (Fig. 1C). There was no significant difference between the proportions of neurons with each sign of response defined by the peak response over the entire trial ($P > 0.30$ for both PPN and STN). We quantified modulation strength using the absolute response change z-scored relative to baseline (Fig. 1D), and found that across all neurons PPN modulation magnitudes were significantly greater during the visual stimulus (PPN-STN = 0.541, SE = 0.264, $P < 0.05$) and imaginary gait (PPN-STN = 0.190, SE = 0.080, $P < 0.05$) epochs. PPN and STN modulation magnitudes did not differ during the button presses initiating and terminating imaginary gait (PPN-STN = 0.085, SE = 0.106, $P > 0.4$).

Individual neurons could exhibit modulation during one or more epochs of the imaginary gait task. We observed that the proportion of neurons modulated during at least one of three epochs (Fig. 1E; Visual, Motor, Imaginary gait) was significantly greater in the PPN compared to STN [57.1% versus 26.9%, 95% confidence interval (CI) for difference = 11.1–49.5, $P < 0.01$]. In addition, significantly task-related neurons more frequently exhibited joint modulation in two or three of task epochs in the PPN compared to the STN (62.5% versus 30.2%, 95% CI for difference = 2.12–58.9, $P < 0.05$).

The location of each single- or multi-unit activity is illustrated in Fig. 2. We did not find any difference between the spatial distributions of task-related neurons compared to those without significant modulations (Fig. 2A) in either the PPN or the STN (P-values > 0.10). Nor did we find evidence of spatial clustering when comparing spatial distributions of neurons modulated in the visual, motor or imaginary gait epochs (Fig. 2B) in either the PPN (P-values > 0.09) or the STN (P-values > 0.5). This lack of difference is perhaps unsurprising in the PPN, where many individual neurons were modulated by more than one task event.

PPN local field potentials exhibit distinct temporally and spatially localized frequency modulations

We further explored PPN activity during imaginary gait by recording local field potentials from the definitive DBS macroelectrodes in a postsurgical session (Fig. 3A). Patients performed the same imaginary gait task as they did intrasurgically, with two additional conditions where they imagined an object moving down the corridor at the two different speeds (normal and rapid). We estimated spectrograms grouping bipolar pairs across patients by relative recording depth (Fig. 3B). PPN local field potentials exhibited robust changes in spectral power that depended on both task events and depth within the nucleus. Following visual instruction onset, we observed transient increases in theta (4–8 Hz), alpha (8–13 Hz), beta (13–30 Hz) and gamma (30–100 Hz) power. These increases were spatially localized, with those in the theta, beta and gamma bands largest at the intermediate dipole, and those in the alpha band equally strong at the dorsal and intermediate dipoles but diminishing significantly at the ventral dipole (P-values < 0.001, see also Supplementary Table 1).

Aligning to the button presses that initiated and terminated imagery revealed that power modulations in all frequency bands were also greatest at the intermediate dipole (P-values < 0.001). During imagination, sustained changes in theta, alpha and beta power were also significantly spatially localized; theta power decreased at all dipoles with the smallest decrease at the intermediate dipole, alpha power increased maximally at the intermediate dipole, while beta power increased maximally at the dorsal and intermediate dipoles (P-values < 0.001). Gamma band power increased at the initiation of imagination, but then decreased below baseline in a non-spatially localized manner until imagery ended, although this

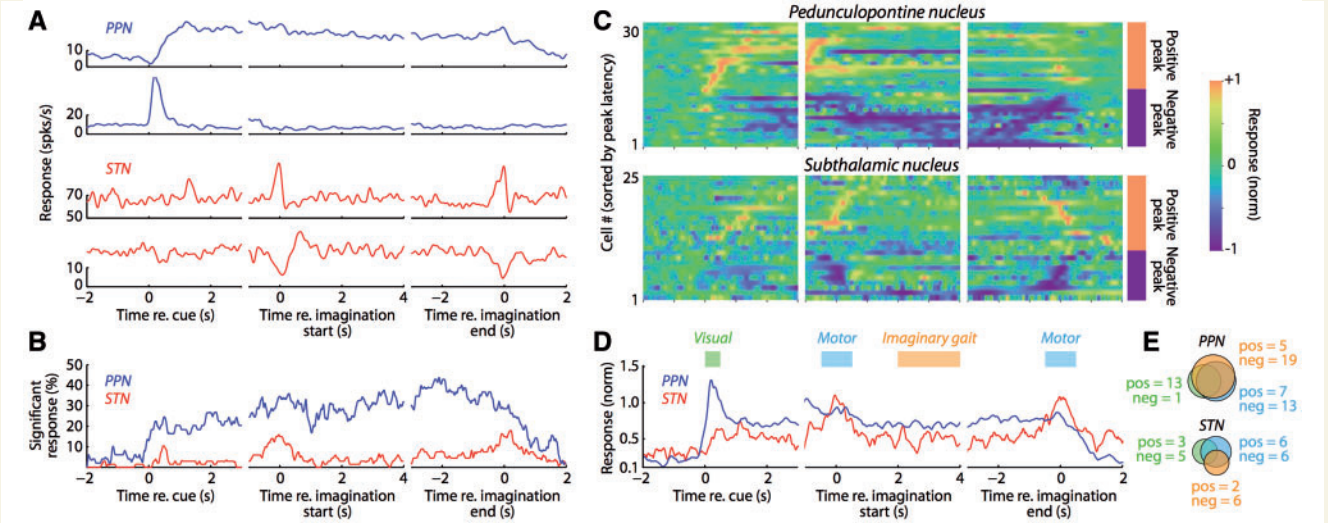

Figure 1 Neural responses in the human PPN and STN during imaginary gait. (**A**) Example PPN and STN activity. Each row represents a different neuron, with each column illustrating activity aligned to one of three different trial events. Activity was smoothed with an optimal Gaussian kernel and averaged over trials. We pooled data from normal and rapid gait imagination since we did not observe any differences between these conditions. (**B**) The PPN is more responsive than the STN during the imaginary gait task. For each neuron, we compared activity at each point in time with the baseline activity of that neuron taken before the presentation of the instruction cue. Significance was pooled across all neural responses after FDR correction, and smoothed with a 50 ms moving average. (**C**) Individual activity profiles for significantly modulated neural responses. All neurons that were significantly modulated relative to baseline are plotted, aligning to the same events as **A** and **B**. The activity for each neural response is smoothed with an optimal Gaussian kernel and normalized to the peak absolute response across the entire trial. In each panel, the neural responses are sorted according to the time of the peak absolute response (separately for positive and negative peak responses). The sign of the peak absolute response is indicated to the right of the last column. (**D**) The PPN and STN respond differently during imaginary gait. Population activity profile including all neurons that were significantly modulated relative to baseline. Neural activity was z-scored relative to baseline before averaging the absolute response. (**E**) Neural responses in the PPN more frequently occur to different task epochs than those in the STN. Individual neural responses were tested for significant differences during three different epochs (indicated in **D**): (i) Visual, corresponding to the presentation of the instruction cue (green); (ii) Motor, corresponding to the overt button presses that indicated the beginning and end of imaginary gait (blue); and (iii) Imaginary gait, when patients had their eyes closed and were imagining walking (orange). 'Pos' and 'neg' indicate the number of neurons exhibiting positive or negative modulations of activity for each epoch.

decrease did not reach significance ($P = 0.0674$). Thus, while visual instruction and physical movement were associated with spatially and temporally localized broadband increases in power, mental imagery was associated with spatially localized sustained increases in power specifically in the alpha and beta bands, with suppression elsewhere. Local field potential power changes were similar during both imaginary gait and imaginary object movement, and none of the changes in theta, alpha, beta or gamma band power depended on the type of imagination (gait or object) or speed (normal or rapid) in any of the visual, motor or imagination epochs (P-values > 0.10).

Discussion

We used locomotor imagery to explore the different contributions of the PPN and STN in human gait. Our study has two important strengths. First, we recruited homogeneous populations of patients with idiopathic Parkinson's disease, with the only notable difference between the two surgical groups being the severity of dopamine-resistant gait and balance disorders. All patients were cognitively normal and extensively trained, ensuring reliable performance of the motor imagery tasks, which required focus, particularly in the operating room. Second, we used an imaginary gait task that has been validated in imaging studies of healthy subjects (Jahn *et al.*, 2008; Karachi *et al.*, 2012) and patients with Parkinson's disease (Snijders *et al.*, 2011; Crémers *et al.*, 2012). This task has separable phases allowing us to correlate neural activity with distinct events. We found that both the PPN and STN were modulated during motor imagery, but the prevalence of PPN modulations spanning multiple events supports the hypothesis that the PPN, but not the STN, likely integrates multiple sources of information to influence locomotor behaviour in humans.

It is important to consider the limitations of comparing the brain activity of two different patient groups. At our centre, STN-DBS is contraindicated by severe DOPA-resistant gait disorders. We note that patients in both the PPN-DBS and STN-DBS groups exhibit gait and balance disorders. These disorders are alleviated by DOPA-

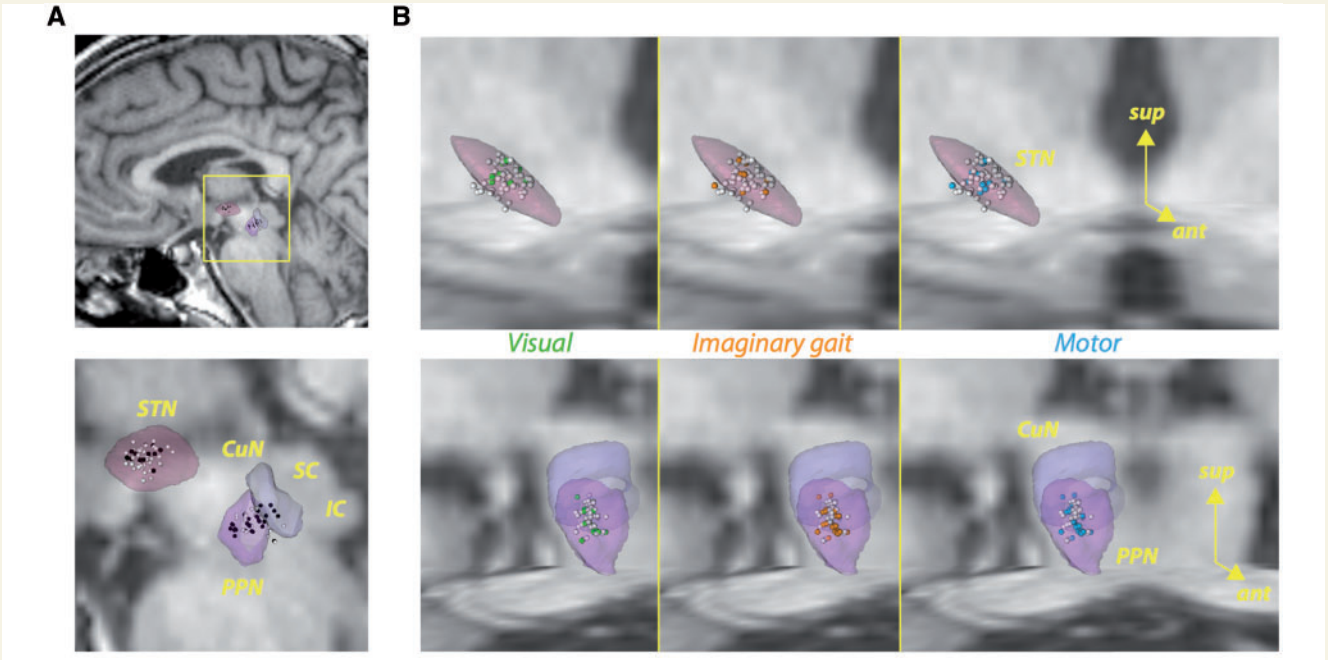

Figure 2 Localization of neurons in the STN and PPN. (**A**) Sagittal views of task-related (black) and non-task-related (white) neurons. (**B**) Localization within the STN (*top row*) or cuneiform nucleus (CuN)/PPN (*bottom row*) of neurons with significant modulations in activity during visual instruction (first column, green spheres), imaginary gait (second column, orange spheres), and button press (third column, blue spheres). White spheres represent the remaining neurons. The STN and CuN/PPN figures include axial and coronal T_1-weighted MRI sections of the histological atlas of Yelnik *et al.* (2007). IC = inferior colliculus; SC = superior colliculus.

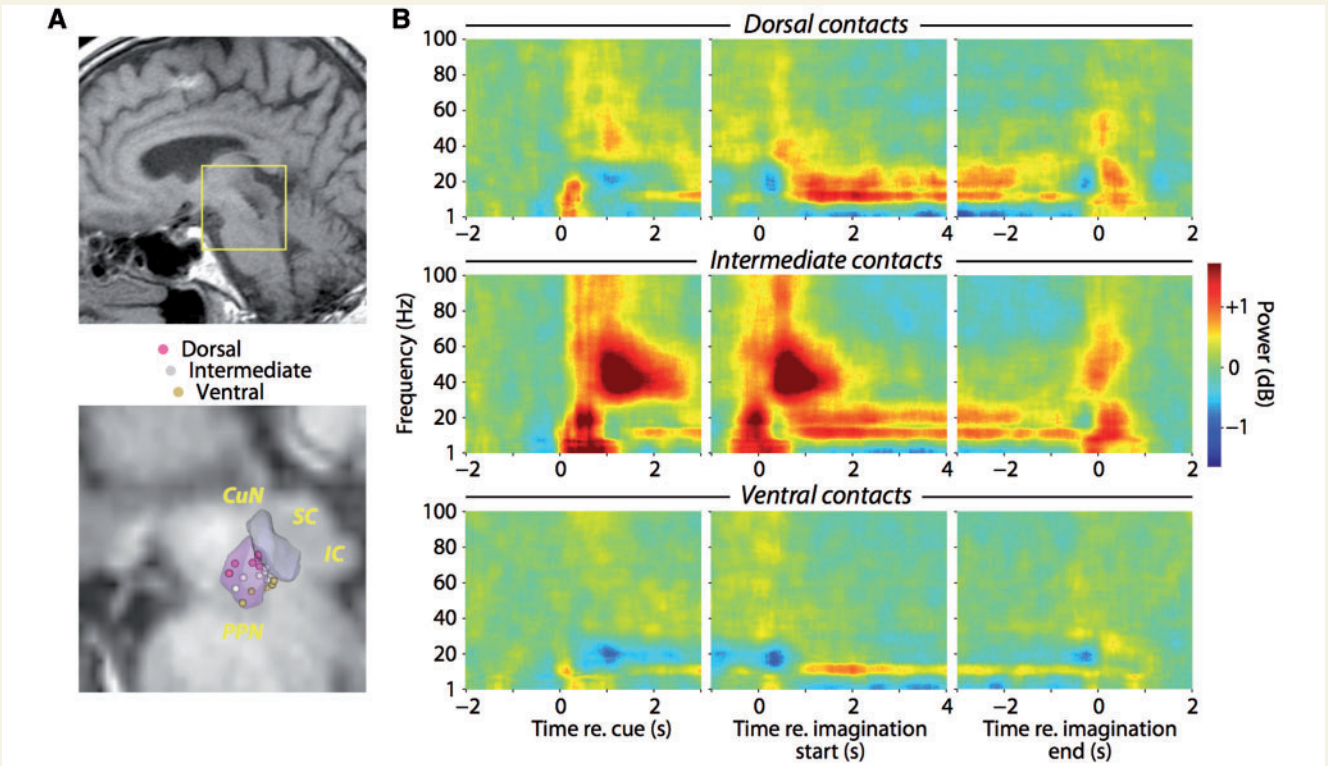

Figure 3 Task-related local field potential activity is spatially localized within the PPN. (**A**) Sagittal view of post-surgical localization of PPN electrodes in T_1-weighted MRI image from one patient (*top*). Illustration of dipole centres for all patients in the histological atlas of Yelnik *et al.* (2007) (*bottom*). Each sphere represents the midway point between adjacent contacts contributing to each bipolar recording. (**B**) Spectrograms of local field potentials recorded from definitive DBS contacts. Recordings from each patient were averaged by dorsal-ventral arrangement along the electrode shaft (*rows*). The panels within each row are aligned to presentation of the visual instruction cue, initiation and termination of imaginary gait. Spectral power is normalized relative to prestimulus power (−3 to −1 s before instruction onset). IC = inferior colliculus; SC = superior colliculus.

therapy in both groups, although the PPN group exhibited significantly more severe DOPA-resistant gait symptoms. It is ours and others experience that most patients with Parkinson's disease eventually develop DOPA-resistant gait and balance disorders, with these disorders signifying the evolution of the same disease (Grabli *et al.*, 2012). This suggests that the STN-DBS group is a reasonable comparison group for the PPN-DBS patients. The differences in real gait led us to use a locomotor imagery task, a useful paradigm in part because patients with Parkinson's disease have preserved locomotor imagery (Snijders *et al.*, 2011; Crémers *et al.*, 2012), despite being impaired during actual movements. Thus we are not comparing activity related to abnormal movements, but rather to processes related to locomotor imagery that are preserved in both patient groups. Indeed, despite differences in real gait between the PPN and STN cohorts, there was no difference in the duration of imaginary gait between PPN and STN groups, nor was there any correlation between step length during real gait and the duration of imaginary gait. This suggests that while the cohorts differed in terms of real gait, they performed locomotor imagery similarly, suggesting our conclusions are reasonable in the context of previous work in healthy humans and animal models discussed in detail below.

We found that the majority of PPN neurons were modulated during imaginary gait. Our post-surgical recordings further revealed that changes in spiking activity were paralleled by sustained increases in alpha- and beta-band power in the PPN during imaginary gait. These changes in spiking and local field potential activity may be relevant for real gait, strengthening observations that mimicking stepping with alternating movements of the legs (passive or active) during DBS surgery (Piallat *et al.*, 2009; Tattersall *et al.*, 2014) and locomotion in animals (Garcia-Rill *et al.*, 1983; Lee *et al.*, 2014) can elicit activity changes in PPN neurons. Furthermore, in patients with Parkinson's disease, prominent alpha-band oscillations within the PPN (Androulidakis *et al.*, 2008) are enhanced during stepping in place (Fraix *et al.*, 2013) and correlate with speed during actual walking (Thevathasan *et al.*, 2012). Our results agree on certain points with the recent report by Tattersall *et al.* (2014), who also observed that the majority of PPN neurons are modulated during imaginary gait. However, they did not find that imagery modulated alpha- or beta-band oscillations, which contrasts with our observations of sustained power increases in these frequency bands. This difference may be due to targeting differences, as we showed that task-related modulations are spatially restricted within the PPN. Taken together, these results suggest that the PPN area is normally active during locomotion in humans. The specific roles remain unclear, although functions including motor planning and attention that are common to both real and imaginary gait are likely possibilities.

Our data support the hypothesis that the PPN may be an appropriate DBS target for treating DOPA-resistant gait disorders. We demonstrated a marked spatial specificity of task-related responses during locomotor imagery within the PPN, which may be useful for targeting this structure during surgery as it has poorly defined boundaries that are not visible using current imaging techniques. Moreover, the diversity of responses in the PPN suggests that DBS of this area likely influences a wide range of functions, which may account for the heterogeneity of clinical results from PPN-DBS obtained thus far. Currently, the best strategy for selecting patients that could benefit from PPN-DBS remains unknown. Low-frequency stimulation of the PPN is thought to activate neurons, and one possibility is that PPN-DBS is effective in those patients with less severe degeneration of the PPN cholinergic neurons. It will be important in the future to understand the relationship between preserved cholinergic function and PPN-DBS effectiveness.

The PPN modulations we observed are potentially related to processes common to both gait and visuomotor imagery. Indeed, we did not observe significant differences in PPN spiking activity according to changes in imaginary gait speed, nor did we observe significant differences in local field potential modulations between imaginary gait and object motion. This raises the intriguing possibility that PPN activity changes signify processes including visual or kinaesthetic imagery, or sustained attention (Kinomura *et al.*, 1996; Paus *et al.*, 1997; Androulidakis *et al.*, 2008) involved in imagining movement. This is in line with evidence implicating the PPN in a number of general functions, including regulating arousal and sleep (Steriade and McCarley, 1990; Urbano *et al.*, 2012) and linking appetitive and aversive outcomes with behavioural responses (Bechara and van der Kooy, 1989; Winn, 2008; Okada and Kobayashi, 2013; Hong and Hikosaka, 2014), which may be mediated via rich connectivity with non-motor brain areas (Chiba *et al.*, 2001). For example, manipulating mesencephalic locomotor region activity can induce startle and escape responses in addition to locomotion (Mori *et al.*, 1989; Condé *et al.*, 1998), and PPN lesions can disrupt performance in certain associative learning tasks despite leaving abilities such as feeding and basic movement intact (Condé *et al.*, 1998; Winn, 2008). These results indicate that PPN functions extend beyond driving locomotor pattern generation or regulating postural tonus, and suggest that the PPN supports processes that are necessary for adaptive locomotion but that may not be gait-specific *per se*.

We also showed, for the first time in humans to our knowledge, that PPN neurons can be strongly activated by visual stimuli, which in our case were task instructions. In postsurgical recordings, these visual stimuli induced transient broad-band changes in local field potential power that extended well into the gamma band. Similarly sharp responses have been observed in the PPN of monkeys performing visually guided saccades (Okada and Kobayashi, 2009; Hong and Hikosaka, 2014), and may be mediated by direct projections from cortical areas such as the frontal

or supplementary eye fields (Matsumura *et al.*, 2000), or from subcortical structures like the superior colliculus (Redgrave *et al.*, 1988). These visual responses appeared distinct from overt motor modulations, which we also observed in spiking activity and local field potentials during button pressing, in agreement with observations that PPN neurons can be modulated during movements outside of any locomotor context (Matsumura *et al.*, 1997; Weinberger *et al.*, 2008; Okada and Kobayashi, 2009; Shimamoto *et al.*, 2010; Tsang *et al.*, 2010; Thompson and Felsen, 2013; Hong and Hikosaka, 2014; Tattersall *et al.*, 2014). PPN visual activity may play a role in increasing alertness or attention to visual stimuli relevant for task performance by influencing cortical processing via ascending projections (Steriade and McCarley, 1990; Lee *et al.*, 2014). These ascending projections may account for reports that PPN-DBS patients experience enhanced alertness during stimulation (Stefani *et al.*, 2013). Such a function likely extends beyond the visual modality, as PPN neurons can also be modulated at short latency by auditory (Reese *et al.*, 1995; Dormont *et al.*, 1998), vestibular (Aravamuthan and Angelaki, 2012), nociceptive (Carlson *et al.*, 2004) and somatosensory (Yeh *et al.*, 2010) stimuli, suggesting that this structure integrates a variety of ongoing sensory information that may be useful for adapting locomotor behaviour to environmental demands (Rossignol *et al.*, 2006). Further experiments are necessary to determine whether individual neurons integrate multimodal sensory information, and how these responses are related to preparatory, associative or cognitive processes linking sensory stimuli and movement.

We used a locomotor imagery task with the eyes closed to isolate the activity changes from potentially confounding visual stimuli. Importantly, the visual responses we observed in the PPN when the eyes were open were transient, and we observed task-related changes that were sustained throughout imaginary gait with the eyes closed, well after the transient visual responses. Moreover, our postsurgical recordings showed that sustained task-related changes were primarily in the alpha and beta bands that were spatially localized within the PPN area. Together with the fact that the patients performed the imaginary gait task correctly, these results argue against the interpretation that the activity changes exclusively from closing the eyes. Supporting this are functional imaging results using imaginary gait with the eyes closed showing blood oxygenation level-dependent changes in the PPN area in healthy volunteers (Jahn *et al.*, 2008; Karachi *et al.*, 2012) and patients with Parkinson's disease (Snijders *et al.*, 2011; Crémers *et al.*, 2012). In these experiments, all conditions contrasted were performed with the eyes closed, indicating that the PPN was modulated by locomotor imagery.

The involvement of the STN during gait appears different, with most task-related modulations occurring during button pressing. This agrees with observations that STN neurons are modulated during voluntary movements, which reflects regulation of basal ganglia inhibition around movement initiation (Matsumura *et al.*, 1992; Wichmann *et al.*, 1994; Hutchison *et al.*, 1998; Williams *et al.*, 2005; Hanson *et al.*, 2012). Few STN neurons were modulated during the imaginary gait epoch, suggesting that the STN may not be specifically active during gait, consistent with the lack of STN modulation during functional imaging of imaginary (Snijders *et al.*, 2011; Crémers *et al.*, 2012; Karachi *et al.*, 2012) or real gait (Hanakawa *et al.*, 1999; La Fougère *et al.*, 2010). Note that the STN is active during imaginary arm movements in patients with Parkinson's disease (Kühn *et al.*, 2006), suggesting that we might have observed STN modulation during imaginary gait if this structure is involved during real gait. The fact that we observed little activity in the STN during imaginary gait constitutes indirect evidence that the STN may not be involved in gait *per se*. However, in the locomotor imagery experiments cited above, gait was relatively automatic, with subjects walking or imagining gait at constant speed without obstacles. Thus, we may have observed relatively few responsive STN neurons as our task did not involve motor or cognitive conflict or a need to switch from automatic behaviour, situations that may specifically engage the STN (Aron and Poldrack, 2006; Frank *et al.*, 2007; Isoda and Hikosaka, 2008). Indeed, the STN is differentially activated in Parkinsons's disease patients with freezing of gait (Vercruysse *et al.*, 2014) as well as in patients with Parkinson's disease navigating a virtual environment with cognitive loading that induced motor arrests (Shine *et al.*, 2013). Such complex situations likely arise during natural locomotion, raising the possibility that the PPN and STN can interact during natural locomotor behaviour to adapt automatic gait programs to internal and external needs.

There is strong evidence that the PPN and STN interact. In Parkinson's disease, high frequency STN stimulation (>100 Hz) alleviates dopamine-sensitive motor symptoms (tremor, rigidity and akinesia), likely through a combination of effects local to the STN as well as effects distributed across brain networks (Kringelbach *et al.*, 2007; Lozano and Lipsman, 2013). Curiously, at these frequencies dopamine-resistant gait disorders can be aggravated, whereas reducing the STN stimulation frequency (<100 Hz) can mildly improve these gait disorders while worsening dopamine-sensitive motor symptoms in certain patients (Moreau *et al.*, 2008). The mechanisms underlying this reversal are not understood, but one possibility is that high frequency STN stimulation worsens dopamine-resistant gait disorders in patients with Parkinson's disease by aggravating PPN dysfunction, possibly through direct projections (Lavoie and Parent, 1994; Neagu *et al.*, 2013). Moreover, PPN lesions in parkinsonian monkeys mitigate dopamine-sensitive motor symptoms while at the same time inducing gait disorders (Grabli *et al.*, 2013). These results highlight a close relationship between these two nuclei in Parkinson's disease, and suggest that the PPN and STN likely interact during natural locomotion, perhaps providing a route for the state of the locomotor system to influence the basal ganglia.

Acknowledgements

We are grateful to the patients for their participation. We thank Dr S. Gallais for managing the anaesthesiology; A. Buot, A. Demain, A. El Helou, C. Ewenczyk, V. Marchal and J. Sellers for training the patients and help collecting the data; and Drs C. François and J. Yelnik for feedback and help in targeting the PPN.

Funding

This study was supported by the Institut National de la Santé et de la Recherche Médicale et Direction Générale de l'Organisation des Soins (INSERM-DGOS), a grant from the Thierry and Annick Desmarest Foundation to C.K. and B.L., an ATIP-Avenir grant and a grant from the Mairie de Paris to B.L., and a grant from the Régie Autonome des Transports Parisiens (RATP) to M.L.W.

Supplementary material

Supplementary material is available at *Brain* online.

References

Androulidakis AG, Mazzone P, Litvak V, Penny W, Dileone M, Gaynor LMFD, et al. Oscillatory activity in the pedunculopontine area of patients with Parkinson's disease. Exp Neurol 2008; 211: 59–66.

Aravamuthan BR, Angelaki DE. Vestibular responses in the macaque pedunculopontine nucleus and central mesencephalic reticular formation. Neuroscience 2012; 223: 183–99.

Aron AR, Poldrack RA. Cortical and subcortical contributions to Stop signal response inhibition: role of the subthalamic nucleus. J Neurosci 2006; 26: 2424–33.

Bakker M, de Lange FP, Stevens JA, Toni I, Bloem BR. Motor imagery of gait: a quantitative approach. Exp Brain Res 2007; 179: 497–504.

Bardinet E, Bhattacharjee M, Dormont D, Pidoux B, Malandain G, Schüpbach M, et al. A three-dimensional histological atlas of the human basal ganglia. II. Atlas deformation strategy and evaluation in deep brain stimulation for Parkinson disease. J Neurosurg 2009; 110: 208–19.

Bechara A, van der Kooy D. The tegmental pedunculopontine nucleus: a brain-stem output of the limbic system critical for the conditioned place preferences produced by morphine and amphetamine. J Neurosci 1989; 9: 3400–9.

Bejjani BP, Dormont D, Pidoux B, Yelnik J, Damier P, Arnulf I, et al. Bilateral subthalamic stimulation for Parkinson's disease by using three-dimensional stereotactic magnetic resonance imaging and electrophysiological guidance. J Neurosurg 2000; 92: 615–25.

Benjamini Y, Hochberg Y. Controlling the False Discovery Rate: A Practical and Powerful Approach to Multiple Testing. J R Stat Soc Ser B 1995; 57: 289–300.

Bohnen NI, Müller MLTM, Koeppe RA, Studenski SA, Kilbourn MA, Frey KA, et al. History of falls in Parkinson disease is associated with reduced cholinergic activity. Neurology 2009; 73: 1670–6.

Carlson JD, Iacono RP, Maeda G. Nociceptive excited and inhibited neurons within the pedunculopontine tegmental nucleus and cuneiform nucleus. Brain Res 2004; 1013: 182–7.

Chiba T, Kayahara T, Nakano K. Efferent projections of infralimbic and prelimbic areas of the medial prefrontal cortex in the Japanese monkey, Macaca fuscata. Brain Res 2001; 888: 83–101.

Condé H, Dormont JF, Farin D. The role of the pedunculopontine tegmental nucleus in relation to conditioned motor performance in the cat. II. Effects of reversible inactivation by intracerebral microinjections. Exp Brain Res 1998; 121: 411–8.

Crémers J, D'Ostilio K, Stamatakis J, Delvaux V, Garraux G. Brain activation pattern related to gait disturbances in Parkinson's disease. Mov Disord 2012; 27: 1498–505.

Demain A, Westby GWM, Fernandez-Vidal S, Karachi C, Bonneville F, Do MC, et al. High-level gait and balance disorders in the elderly: a midbrain disease? J Neurol 2014; 261: 196–206.

Dormont JF, Condé H, Farin D. The role of the pedunculopontine tegmental nucleus in relation to conditioned motor performance in the cat. I. Context-dependent and reinforcement-related single unit activity. Exp Brain Res 1998; 121: 401–10.

Eidelberg E, Walden JG, Nguyen LH. Locomotor control in macaque monkeys. Brain 1981; 104: 647–63.

Ferraye MU, Debû B, Fraix V, Goetz L, Ardouin C, Yelnik J, et al. Effects of pedunculopontine nucleus area stimulation on gait disorders in Parkinson's disease. Brain 2010; 133: 205–14.

La Fougère C, Zwergal A, Rominger A, Förster S, Fesl G, Dieterich M, et al. Real versus imagined locomotion: a [18F]-FDG PET-fMRI comparison. Neuroimage 2010; 50: 1589–98.

Fraix V, Bastin J, David O, Goetz L, Ferraye M, Benabid A-L, et al. Pedunculopontine nucleus area oscillations during stance, stepping and freezing in Parkinson's disease. PLoS One 2013; 8: e83919.

Frank MJ, Samanta J, Moustafa AA, Sherman SJ. Hold your horses: impulsivity, deep brain stimulation, and medication in parkinsonism. Science 2007; 318: 1309–12.

Garcia-Rill E, Skinner RD, Fitzgerald JA. Activity in the mesencephalic locomotor region during locomotion. Exp Neurol 1983; 82: 609–22.

Grabli D, Karachi C, Folgoas E, Monfort M, Tande D, Clark S, et al. Gait disorders in parkinsonian monkeys with pedunculopontine nucleus lesions: a tale of two systems. J Neurosci 2013; 33: 11986–93.

Grabli D, Karachi C, Welter M-L, Lau B, Hirsch EC, Vidailhet M, et al. Normal and pathological gait: what we learn from Parkinson's disease. J Neurol Neurosurg Psychiatry 2012; 83: 979–85.

Hanakawa T, Katsumi Y, Fukuyama H, Honda M, Hayashi T, Kimura J, et al. Mechanisms underlying gait disturbance in Parkinson's disease: a single photon emission computed tomography study. Brain 1999; 122: 1271–82.

Hanson TL, Fuller AM, Lebedev MA, Turner DA, Nicolelis MAL. Subcortical neuronal ensembles: an analysis of motor task association, tremor, oscillations, and synchrony in human patients. J Neurosci 2012; 32: 8620–32.

Hirsch EC, Graybiel AM, Duyckaerts C, Javoy-Agid F. Neuronal loss in the pedunculopontine tegmental nucleus in Parkinson disease and in progressive supranuclear palsy. Proc Natl Acad Sci USA 1987; 84: 5976–80.

Hong S, Hikosaka O. Pedunculopontine tegmental nucleus neurons provide reward, sensorimotor, and alerting signals to midbrain dopamine neurons. Neuroscience 2014; 282: 139–55.

Hutchison WD, Allan RJ, Opitz H, Levy R, Dostrovsky JO, Lang AE, et al. Neurophysiological identification of the subthalamic nucleus in surgery for Parkinson's disease. Ann Neurol 1998; 44: 622–8.

Isoda M, Hikosaka O. Role for subthalamic nucleus neurons in switching from automatic to controlled eye movement. J Neurosci 2008; 28: 7209–18.

Jahn K, Deutschländer A, Stephan T, Kalla R, Wiesmann M, Strupp M, et al. Imaging human supraspinal locomotor centers in brainstem and cerebellum. Neuroimage 2008; 39: 786–92.

Jellinger K. The pedunculopontine nucleus in Parkinson's disease, progressive supranuclear palsy and Alzheimer's disease. J Neurol Neurosurg Psychiatry 1988; 51: 540–3.
Karachi C, André A, Bertasi E, Bardinet E, Lehéricy S, Bernard FA. Functional parcellation of the lateral mesencephalus. J Neurosci 2012; 32: 9396–401.
Karachi C, Grabli D, Bernard FA, Tandé D, Wattiez N, Belaid H, et al. Cholinergic mesencephalic neurons are involved in gait and postural disorders in Parkinson disease. J Clin Invest 2010; 120: 2745–54.
Kinomura S, Larsson J, Gulyás B, Roland PE. Activation by attention of the human reticular formation and thalamic intralaminar nuclei. Science 1996; 271: 512–5.
Kringelbach ML, Jenkinson N, Owen SLF, Aziz TZ. Translational principles of deep brain stimulation. Nat Rev Neurosci 2007; 8: 623–35.
Kühn AA, Doyle L, Pogosyan A, Yarrow K, Kupsch A, Schneider G-H, et al. Modulation of beta oscillations in the subthalamic area during motor imagery in Parkinson's disease. Brain 2006; 129: 695–706.
Lavoie B, Parent A. Pedunculopontine nucleus in the squirrel monkey: projections to the basal ganglia as revealed by anterograde tract-tracing methods. J Comp Neurol 1994; 344: 210–31.
Lee AM, Hoy JL, Bonci A, Wilbrecht L, Stryker MP, Niell CM. Identification of a brainstem circuit regulating visual cortical state in parallel with locomotion. Neuron 2014; 83: 455–66.
Limousin P, Krack P, Pollak P, Benazzouz A, Ardouin C, Hoffman D, et al. Electrical stimulation of the subthalamic nucleus in advanced Parkinson's disease. N Engl J Med 1998; 339: 1105–11.
Lozano AM, Lipsman N. Probing and regulating dysfunctional circuits using deep brain stimulation. Neuron 2013; 77: 406–24.
Maillet A, Thobois S, Fraix V, Redouté J, Le Bars D, Lavenne F, et al. Neural substrates of levodopa-responsive gait disorders and freezing in advanced Parkinson's disease: a kinesthetic imagery approach. Hum Brain Mapp 2015; 36: 959–80.
Matsumura M, Kojima J, Gardiner TW, Hikosaka O. Visual and oculomotor functions of monkey subthalamic nucleus. J Neurophysiol 1992; 67: 1615–32.
Matsumura M, Nambu A, Yamaji Y, Watanabe K, Imai H, Inase M, et al. Organization of somatic motor inputs from the frontal lobe to the pedunculopontine tegmental nucleus in the macaque monkey. Neuroscience 2000; 98: 97–110.
Matsumura M, Watanabe K, Ohye C. Single-unit activity in the primate nucleus tegmenti pedunculopontinus related to voluntary arm movement. Neurosci Res 1997; 28: 155–65.
Mazzone P, Lozano A, Stanzione P, Galati S, Scarnati E, Peppe A, et al. Implantation of human pedunculopontine nucleus: a safe and clinically relevant target in Parkinson's disease. Neuroreport 2005; 16: 1877–81.
Mitra P, Bokil H. Observed brain dynamics. New York: Oxford University Press; 2007.
Moreau C, Defebvre L, Destée a, Bleuse S, Clement F, Blatt JL, et al. STN-DBS frequency effects on freezing of gait in advanced Parkinson disease. Neurology 2008; 71: 80–4.
Mori S, Sakamoto T, Ohta Y, Takakusaki K, Matsuyama K. Site-specific postural and locomotor changes evoked in awake, freely moving intact cats by stimulating the brainstem. Brain Res 1989; 505: 66–74.
Moro E, Hamani C, Poon Y-Y, Al-Khairallah T, Dostrovsky JO, Hutchison WD, et al. Unilateral pedunculopontine stimulation improves falls in Parkinson's disease. Brain 2010; 133: 215–24.
Neagu B, Tsang E, Mazzella F, Hamani C, Moro E, Hodaie M, et al. Pedunculopontine nucleus evoked potentials from subthalamic nucleus stimulation in Parkinson's disease. Exp Neurol 2013; 250: 221–7.
Okada KI, Kobayashi Y. Characterization of oculomotor and visual activities in the primate pedunculopontine tegmental nucleus during visually guided saccade tasks. Eur J Neurosci 2009; 30: 2211–23.
Okada KI, Kobayashi Y. Reward prediction-related increases and decreases in tonic neuronal activity of the pedunculopontine tegmental nucleus. Front Integr Neurosci 2013; 7: 36.
Olszewski J, Baxter D. Cytoarchitecture of the human brain stem. Philadelphia: Lippincott; 1954.
Orlovsky G, Deliagina T, Grillner S. Neural Control of Locomotion: from Mollusc to Man. London: Oxford University Press; 1999.
Pahapill PA, Lozano AM. The pedunculopontine nucleus and Parkinson's disease. Brain 2000; 123 (Pt 9): 1767–83.
Paus T, Zatorre RJ, Hofle N, Caramanos Z, Gotman J, Petrides M, et al. Time-related changes in neural systems underlying attention and arousal during the performance of an auditory vigilance task. J Cogn Neurosci 1997; 9: 392–408.
Piallat B, Chabardès S, Torres N, Fraix V, Goetz L, Seigneuret E, et al. Gait is associated with an increase in tonic firing of the sub-cuneiform nucleus neurons. Neuroscience 2009; 158: 1201–5.
Plaha P, Gill SS. Bilateral deep brain stimulation of the pedunculopontine nucleus for Parkinson's disease. Neuroreport 2005; 16: 1883–7.
Le Ray D, Juvin L, Ryczko D, Dubuc R. Supraspinal control of locomotion: the mesencephalic locomotor region. Prog Brain Res 2011; 188: 51–70.
Redgrave P, Dean P, Mitchell IJ, Odekunle A, Clark A. The projection from superior colliculus to cuneiform area in the rat. I. Anatomical studies. Exp Brain Res 1988; 72: 611–25.
Reese NB, Garcia-Rill E, Skinner RD. Auditory input to the pedunculopontine nucleus: II. Unit responses. Brain Res Bull 1995; 37: 265–73.
Rolland AS, Karachi C, Muriel MP, Hirsch EC, François C. Internal pallidum and substantia nigra control different parts of the mesopontine reticular formation in primate. Mov Disord 2011; 26: 1648–56.
Rossignol S, Dubuc R, Gossard JP. Dynamic sensorimotor interactions in locomotion. Physiol Rev 2006; 86: 89–154.
Shik M, Severin F, Orlovsky G. Control of walking and running by means of electric stimulation of the midbrain. Biofizika 1966; 11: 659–66.
Shimamoto SA, Larson PS, Ostrem JL, Glass GA, Turner RS, Starr PA. Physiological identification of the human pedunculopontine nucleus. J Neurol Neurosurg Psychiatry 2010; 81: 80–6.
Shimazaki H, Shinomoto S. Kernel bandwidth optimization in spike rate estimation. J Comput Neurosci 2010; 29: 171–82.
Shine JM, Matar E, Ward PB, Bolitho SJ, Gilat M, Pearson M, et al. Exploring the cortical and subcortical functional magnetic resonance imaging changes associated with freezing in Parkinson's disease. Brain 2013; 136: 1204–15.
Skinner RD, Garcia-Rill E. The mesencephalic locomotor region (MLR) in the rat. Brain Res 1984; 323: 385–9.
Snijders AH, Leunissen I, Bakker M, Overeem S, Helmich RC, Bloem BR, et al. Gait-related cerebral alterations in patients with Parkinson's disease with freezing of gait. Brain 2011; 134: 59–72.
Snijders AH, van de Warrenburg BP, Giladi N, Bloem BR. Neurological gait disorders in elderly people: clinical approach and classification. Lancet Neurol 2007; 6: 63–74.
Stefani A, Lozano AM, Peppe A, Stanzione P, Galati S, Tropepi D, et al. Bilateral deep brain stimulation of the pedunculopontine and subthalamic nuclei in severe Parkinson's disease. Brain 2007; 130: 1596–607.
Stefani A, Peppe A, Galati S, Bassi MS, D'Angelo V, Pierantozzi M. The serendipity case of the pedunculopontine nucleus low-frequency brain stimulation: chasing a gait response, finding sleep, and cognition improvement. Front Neurol 2013; 4: 68.
Steriade M, McCarley R. Brainstem control of wakefulness and sleep. New York: Plenum Press; 1990.
Székely GJ, Rizzo ML. Energy statistics: A class of statistics based on distances. J Stat Plan Inference 2013; 143: 1249–72.
Takakusaki K, Habaguchi T, Ohtinata-Sugimoto J, Saitoh K, Sakamoto T. Basal ganglia efferents to the brainstem centers controlling postural muscle tone and locomotion: a new concept for

understanding motor disorders in basal ganglia dysfunction. Neuroscience 2003; 119: 293–308.
Tattersall TL, Stratton PG, Coyne TJ, Cook R, Silberstein P, Silburn PA, et al. Imagined gait modulates neuronal network dynamics in the human pedunculopontine nucleus. Nat Neurosci 2014; 17: 449–54.
Thevathasan W, Pogosyan A, Hyam JA, Jenkinson N, Foltynie T, Limousin P, et al. Alpha oscillations in the pedunculopontine nucleus correlate with gait performance in parkinsonism. Brain 2012; 135: 148–60.
Thompson JA, Felsen G. Activity in mouse pedunculopontine tegmental nucleus reflects action and outcome in a decision-making task. J Neurophysiol 2013; 110: 2817–29.
Tsang EW, Hamani C, Moro E, Mazzella F, Poon YY, Lozano A. M, et al. Involvement of the human pedunculopontine nucleus region in voluntary movements. Neurology 2010; 75: 950–9.
Urbano FJ, Kezunovic N, Hyde J, Simon C, Beck P, Garcia-Rill E. Gamma band activity in the reticular activating system. Front Neurol 2012; 3: 6.
Vercruysse S, Spildooren J, Heremans E, Wenderoth N, Swinnen SP, Vandenberghe W, et al. The neural correlates of upper limb motor blocks in parkinson's disease and their relation to freezing of gait. Cereb Cortex 2014; 24: 3154–66.
Weinberger M, Hamani C, Hutchison WD, Moro E, Lozano AM, Dostrovsky JO. Pedunculopontine nucleus microelectrode recordings in movement disorder patients. Exp Brain Res 2008; 188: 165–74.
Welter ML, Houeto JL, Tezenas du Montcel S, Mesnage V, Bonnet AM, Pillon B, et al. Clinical predictive factors of subthalamic stimulation in Parkinson's disease. Brain 2002; 125: 575–83.
Wichmann T, Bergman H, DeLong MR. The primate subthalamic nucleus. I. Functional properties in intact animals. J Neurophysiol 1994; 72: 494–506.
Williams ZM, Neimat JS, Cosgrove GR, Eskandar EN. Timing and direction selectivity of subthalamic and pallidal neurons in patients with Parkinson disease. Exp Brain Res 2005; 162: 407–16.
Winn P. Experimental studies of pedunculopontine functions: are they motor, sensory or integrative? Parkinsonism Relat Disord 2008; 14 (Suppl 2): S194–8.
Yeh IJ, Tsang EW, Hamani C, Moro E, Mazzella F, Poon YY, et al. Somatosensory evoked potentials recorded from the human pedunculopontine nucleus region. Mov Disord 2010; 25: 2076–83.
Yelnik J, Bardinet E, Dormont D, Malandain G, Ourselin S, Tandé D, et al. A three-dimensional, histological and deformable atlas of the human basal ganglia. I. Atlas construction based on immunohistochemical and MRI data. Neuroimage 2007; 34: 618–38.
Zanos TP, Mineault PJ, Pack CC. Removal of spurious correlations between spikes and local field potentials. J Neurophysiol 2011; 105: 474–86.
Zrinzo L, Zrinzo L V, Tisch S, Limousin PD, Yousry TA, Afshar F, et al. Stereotactic localization of the human pedunculopontine nucleus: atlas-based coordinates and validation of a magnetic resonance imaging protocol for direct localization. Brain 2008; 131: 1588–98.
Zweig RM, Jankel WR, Hedreen JC, Mayeux R, Price DL. The pedunculopontine nucleus in Parkinson's disease. Ann Neurol 1989; 26: 41–6.